POAC'23
Glasgow, UK

Proceedings of the 27th International Conference on
Port and Ocean Engineering under Arctic Conditions
June 12-16, 2023, Glasgow, UK

An experimental study on the ice fracture behaviors in high-speed water jet-ice interaction considering initial defects in ice

Guangyu Yuan[1,2]; Baoyu Ni[1]*; Wenjun Lu[2]; Zuocheng Wang[1]

1 College of Shipbuilding Engineering, Harbin Engineering University, Harbin 150001, China
2 Department of Civil and Environmental Engineering, Norwegian University of Science and Technology, Trondheim,7034, Norway
Corresponding author Email: nibaoyu@hrbeu.edu.cn

ABSTRACT

A natural ice sheet contains a lot of defects including pre-existing cracks, inclusions, pores, grain boundaries and others. The initial defects have great effects on the properties and mechanical behaviors of the ice sheet, while there are not enough existing researches on defective ice. Yuan et al. (2022) studied the mechanism of ice damage under the action of high-speed water jet with "pure" ice sheet, which experimentally validated the ice-breaking capability of water jet. On this basis, a series of experiments of water jet impacting defective ice were performed in this paper with a purposely designed jet generator and ice samples produced in a cold room, including seven types of initial defects. The entire evolution of the water jet and ice was recorded by two high-speed cameras from the top and front views simultaneously. The focus was the effects of three kinds of initial radial defects and four kinds of initial circumferential defects on the damage and crack propagation of ice plates under high-speed water jet loads. The study provides references for damage analysis of ice with defects under impact loads such as jet flow.

KEY WORDS: Ice; Initial defects, Water jet, Fracture behaviors.

1. INTRODUCTION

Ice breaking has become one of the main problems faced by ships and other equipment operating in the ice-covered waters (Riska, 2011; Xue et al., 2020; Yang et al., 2021). On the basis of conventional ice breaking methods, such as icebreakers, new auxiliary methods (Ni and Wu, 2020; Ni et al., 2023) are always being pursued and studied to improve the ice-breaking capability. Inspired by high-speed water jets' strong damage effect found in other study areas, Yuan et al. (2022) propose a potential ice-breaking method by using the high-speed water jet. In the future, we imagine that the icebreakers will carry high-speed water jet generators to fracture or crack the thick ice in front of the vessel. This will effectively reduce the "ice resistance" for ice-going vessels. Ice breaking by using high-speed water jet is a multiple-interface interaction problem, including water-gas interface and ice-water interface. It presents much challenge to theoretical and numerical studies. Experimental method will be a direct way. On the other hand, shock-wave and bubble jet have been found effective in ice-breaking (Yuan et al., 2020; Ni et al., 2021; 2022), which also lay a strong foundation for ice breaking by using a high-speed water jet.

From an ice mechanics point of view, ice is regarded as one of the most complex materials in nature (Timco and Weeks, 2010). A natural ice sheet contains a lot of defects including pre-existing cracks, inclusions, pores, grain boundaries and others (Geoge, 1986; Grishina and Buch, 2004; (Sanderson 1988, Schulson and Duval 2009)). The defects have great effects on the properties and mechanical behaviors of the ice sheet and make the natural ice sheet difficult to model directly in laboratory (Moslet, 2007; Wang et al., 2019). Li et al. (2010) made some in-situ observations of ice growth and decay processes. According to their study, four kinds of air bubbles were observed in the ice. The size of these air bubbles ranged from 0 mm to 800 mm, and they distributed randomly in the ice. More importantly, these defects have great effect on the property of ice sheet, and cracks are apt to propagate in the area with defects (Moslet, 2007).

In this paper, a series of experiments of water jet impacting defective ice were performed with a purposely-designed jet generator and ice samples produced in a cold room, including seven types of initial defects. The interaction between the water jet and the ice was recorded by two high-speed cameras from the top and front views simultaneously. The focus was the effects of three kinds of initial radial defects and four kinds of initial circumferential defects on the damage and crack propagation of ice plates under high-speed water jet loads. The study could provide references for damage analysis of ice with defects and give better ice-breaking plan under impact loads such as jet flow to show if it is an effective method to improve the ice breaking efficiency to make the initial defect of ice plate artificially.

2. EXPERIMENTAL SET-UP

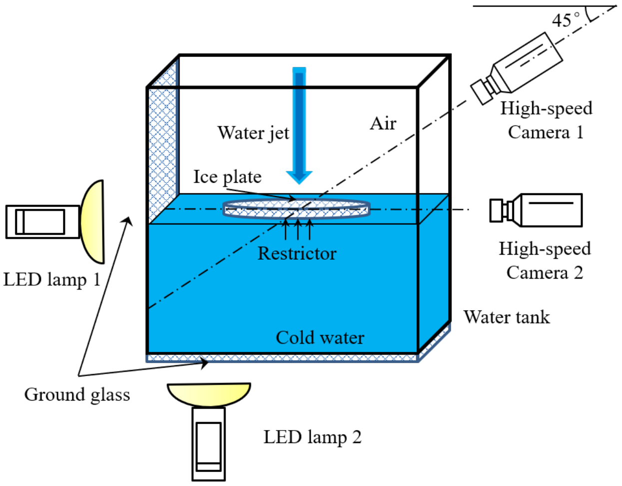

Fig. 1 Experiment set-up

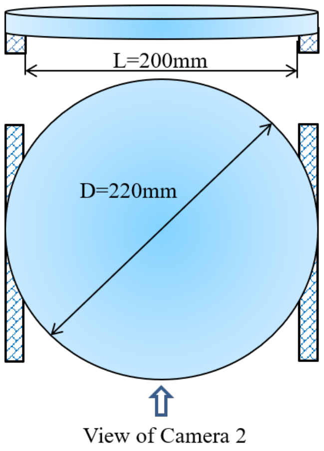

Fig. 2 Sketch of ice plate boundary

In experiments, two high-speed cameras were adopted with synchronous trigger technology. The high-speed camera 1 is Fastcam Mini AX200 and the high-speed camera 2 is Fastcam SA-Z. The vertical cracks of ice plates developed rapidly in the experiments, so most of the experiments in this paper were shot at a rate of 20 000 frames per second for camera 1 and 100 000 frames per second for camera 2. The high-speed water jet with a diameter of 2 mm is generated by a custom-made device (Yuan et al., 2022). The distance between the nozzle and the upper surface of the ice plate is 30 mm, and the water jet slamming velocity is about 112.3

m/s. Due to set-up limitations of the water jet generator, the high-speed camera 1 could not shot the top view of the ice plate vertically downward, we adopted the arrangement method of 45° between the main axis of high-speed camera 1 and the horizontal surface, as shown in Fig. 1. Two cold constant LED light lamps with power of 300 W were adopted and two frosted glasses were arranged on the side and bottom of the transparent water tank to ensure the intensity and uniformity of the lighting.

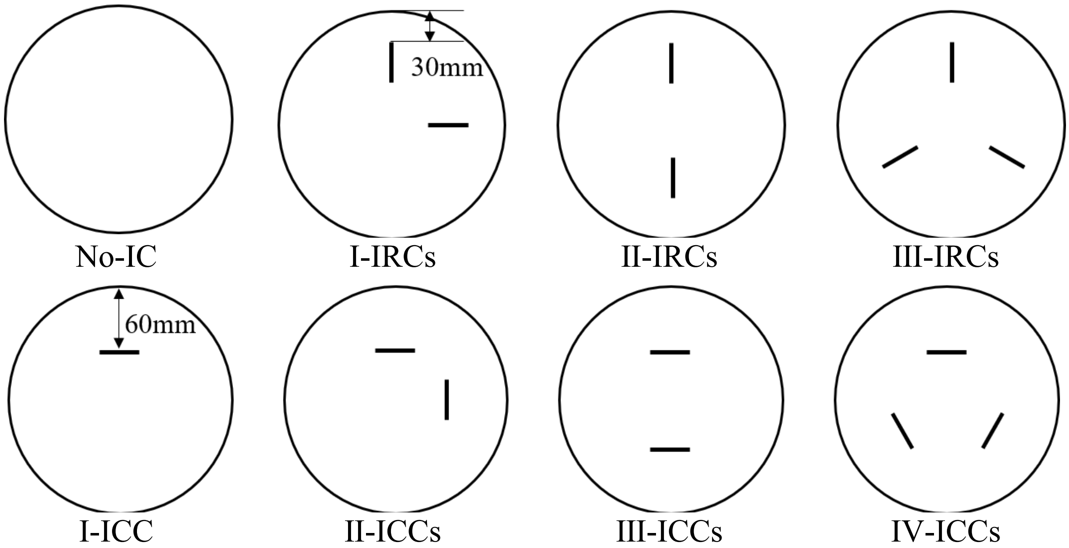

No-IC I-IRCs II-IRCs III-IRCs

I-ICC II-ICCs III-ICCs IV-ICCs

Fig.3 Schematic diagram of initial crack defect layout on the ice plates (Initial crack size: 50 mm × 2 mm; symmetrically distributed along the center of the ice plate; the angle between two adjacent cracks is respectively 90°; 120°; 180°)

The ice plates used in this paper were made of fresh boiled water, the temperature was -5 °C, with the diameter of 220 mm and the thickness of 8 mm. One can refer to Ni et al., 2021 for details on the preparation method of the ice plate and the physical and mechanical properties of freshwater ice at -5 °C. In this paper, the effects of three initial radial defects (I-IRCs; II-IRCs; III-IRCs) and four initial circumferential defects (I-ICC; II-ICCs; III-ICCs; IV-ICCs) on ice damage under water jet load were considered, as shown in Fig. 3. The size of each single initial crack was 50 mm × 2 mm. For initial radial defects, the edge of the crack was 30 mm away from the edge of the ice plate, and for the initial circumferential defect, the center of the crack was 60 mm from the edge of the ice plate. The initial defects symmetrically distributed along the center of the ice plate, and the angle between two adjacent cracks was respectively 90°, 120°, and 180°.

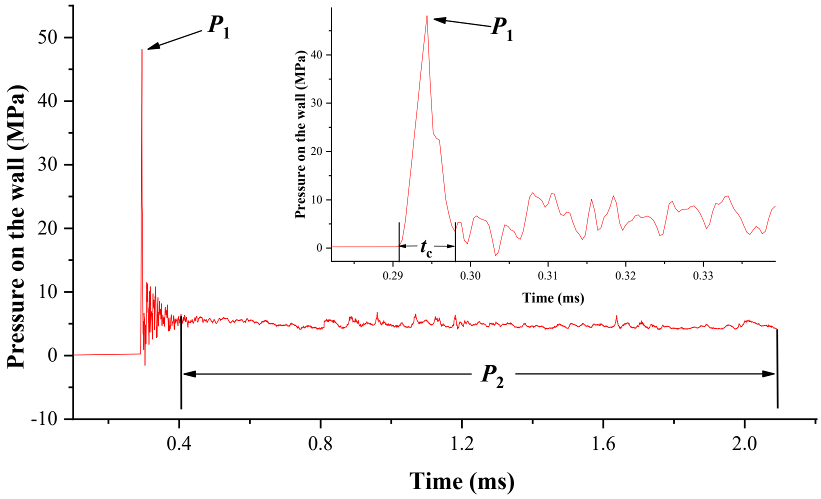

Fig.4 Time history of high-speed water jet pressure on the wall with partial enlargement, t_c=7.6 μs

As a reference, Fig. 4 shows the time history of the pressure of water jet on a rigid wall, with an enlarged view, more information about the measurements of wall pressure please refer to Yuan et al. (2022). Zero time was defined as when the water jet was released. The whole process can be divided into two stages: compressible stage and incompressible stage. In compressible stage, the compressibility of fluid is important and the pressure is very large, while the compressibility of fluid is unimportant and can be ignored in the incompressible stage. The pressure peak in the compressible stage on the wall is defined as “compressible pressure peak P_1”, that is, water hammer pressure, whose value was around 48.25 MPa for this case. Besides, the duration of the main (first) compression pulse (Bowden and Brunton, 1961) is defined as t_c and its value was around 7.6 μs for this case. Compressible stage was followed by incompressible stage. We defined the average of the incompressible pressure in large time on the wall as “stable incompressible pressure P_2”, whose value was around 8.52 MPa for this case.

3．RESULTS AND DISCUSSIONS

3.1 Case with no initial defects in ice

Before studying the damage characteristics of water jet to ice plate with initial defects, firstly, we selected a comparative working condition with no initial defect on the ice plate as examples. This would give us an overview on the interaction process between the water jet and the ice plate.

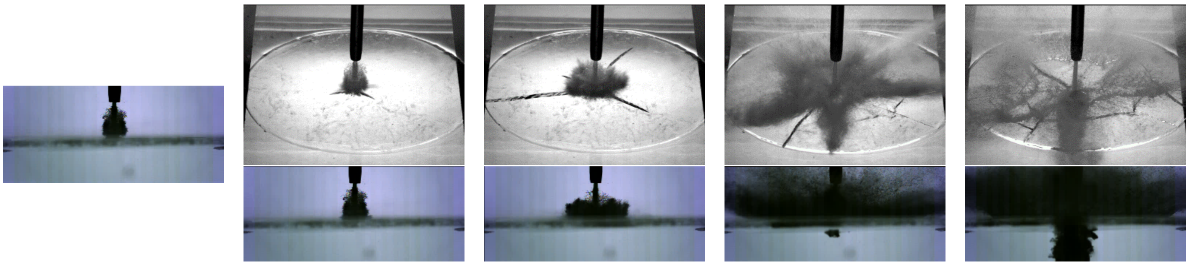

(a) t'=10μs (b) t'=30μs (c) t'=480μs (d)t'=2240μs (t'_{pen}) (e)t'=4080μs (t'_{com})

Fig. 5 Ice plate without initial crack defect

This part mainly studied the damage process of high-speed water jet to the intact ice plate. Initially, under the action of “water hammer pressure” shock waves, the initial radial cracks (RCs) are generated. The cracks first appeared on the lower surface of the ice plate and spread from bottom to top, as shown in Figs. 5 (a). Under the parameters of water jet strength and ice thickness selected in this paper, the “water hammer pressure” caused radial cracks for both the intact ice plate and ice plates with initial defects. However, the damage mechanisms of ‘water hammer pressure’ on ice is not the focus of this article. For interested readers, one can consult to Yuan et al., (2022) on this topic. After that, multiple radial crack (RCs) propagated, and the first radial crack reached the edge of the ice plate in Fig. 5(c). Subsequently, under the “stagnation pressure” of the continuous impact of the water jet, the water jet penetrated the ice plate in Fig. 5(d). This moment was defined as the “penetration time t'_{pen}”. Then, under the action of the top concentrated loads and lower water support, the wedge ice plate generated circumferential cracks (CCs). In Fig. 5(e), all crack propagation was completed, this moment was defined as the “completion time t'_{com}”, and the subsequent water jet energy was transformed into the kinetic energy and potential energy of ice plate fragments. Finally, the ice plate broke into small pieces and flipped over, with a splash of water.

3.2 Cases with three kinds of initial radial defects in ice

As shown as the initial defect diagram in Fig. 3, this part mainly studied the damage of the ice plates with three kinds of initial radial defects under the water jet loads (mainly stagnation pressure, that is the incompressible pressure).

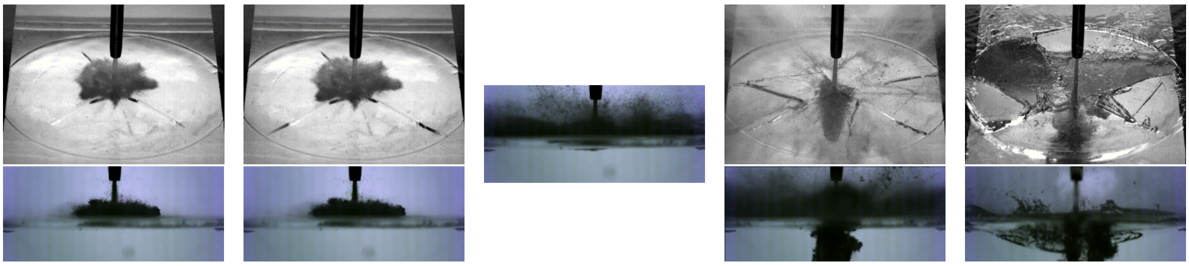

(a) t'=660μs (b) t'=710μs (c) t'=2330μs (t'_{pen}) (d)t'=3910μs (t'_{com}) (e)t'=20010μs

Fig. 6 Ice plate with initial radial defect (I-IRCs)

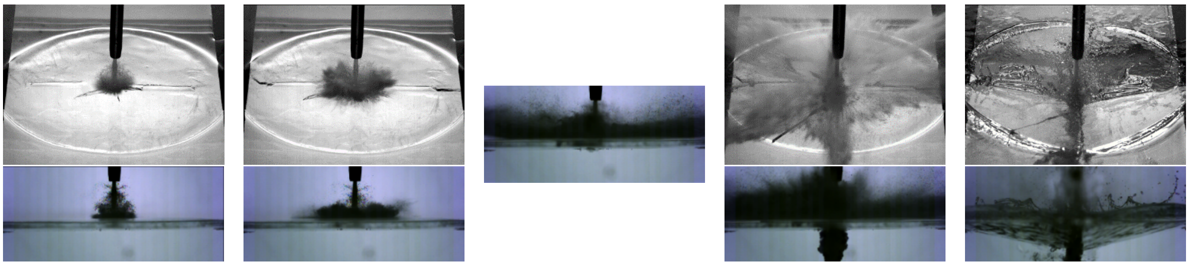

(a) t'=110μs (b) t'=510μs (c) t'=2020μs (t'_{pen}) (d)t'=2660μs (t'_{com}) (e)t'=20010μs

Fig. 7 Ice plate with initial radial defect (II-IRCs)

In Figs. 6 and 7, we analyzed the influence of the initial two radial cracks (I-IRCs and II-IRCs) on the ice plate damage process. First, under the shock waves of the initial compressible pressure, radial cracks were generated by the same principle as intact ice plates in Fig. 5. Then the radial crack first propagated in the direction of the initial defects and connected with them. The cracks appeared at the distal end of the initial defect and extend to the out edge of the ice plate with more radial cracks. Under the continuous impact of the stagnation pressure jet, the jet penetrated the ice plate and generated more radial cracks. Different from the complete ice plate, in this case, almost no circumferential cracks were generated. This was because the ice plate with initial defects had been completely separated under the action of the jet, and more energy of the jet was converted into the mechanical energy of the ice plate fragments. Finally, crack propagation was completed and the ice plate turned over under the action of jet. By comparing Figs 5 to 7, it could be found that the initial defects accelerated the failure process of the ice plate, both t'_{pen} and t'_{com}. At the same time, for the finite size ice plate with two initial defects, the failure process and damage speed of the ice with II-IRCs were faster.

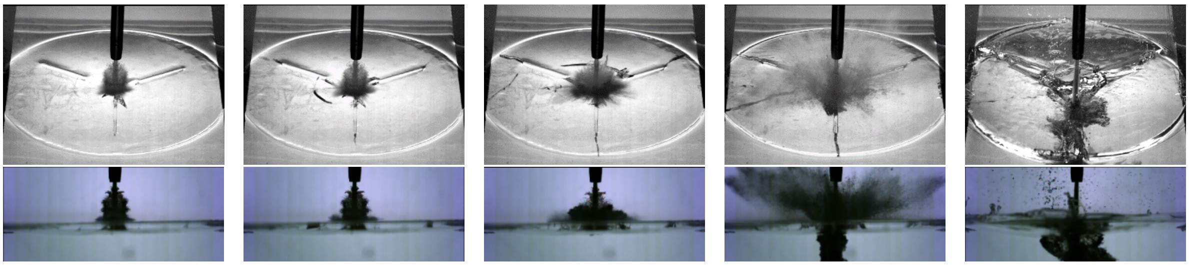

(a) t'=60μs (b) t'=110μs (c) t'=310μs (t'_{pen}) (d)t'=1360μs (t'_{com}) (e)t'=20010μs

Fig. 8 Ice plate with initial radial defect (III-IRCs)

In Fig. 8, we showed a condition with three initial radial defects (III-IRCs). Firstly, the general rule was that with the increase of the number of radial defects, the failure process of finite size ice plate was further accelerated, such as t'_{pen} and t'_{com}. The difference lied in that, for this working condition, partial circumferential cracks appeared along with radial crack propagation along the radial defect, as shown in Fig. 8(b-c). However, it could be found that in the final failure state, as shown in Fig. 8(e), except for the three main radial cracks, the ice plate did not separate along other cracks, which denoted that those cracks were "partially through cracks" (Bazant et al., 1995). More details on partially through cracks can refer to the discussions in Ni et al., (2021). For ice plates of finite size, the main failure mode was driven by radial cracks. This is in accordance to relevant previous theoretical studies e.g., in (Sodhi 1996, Lu, Lubbad et al. 2015) so different initial radial defects could be used to optimized the ice-breaking process and accelerated the separation of ice plates. For example, the small ice sheet could be separated more effectively by presetting multiple initial radial crack defects on the ice sheet, and the ice breaking efficiency can be improved by increasing the number of initial defects and adopting a more rational arrangement of initial defects

3.2 Cases with four kinds of initial circumferential defects in ice

As shown as the initial defect diagram in Fig. 3, this part mainly studied the damage of the ice plates with four kinds of initial circumferential defects under the water jet loads (mainly stagnation pressure).

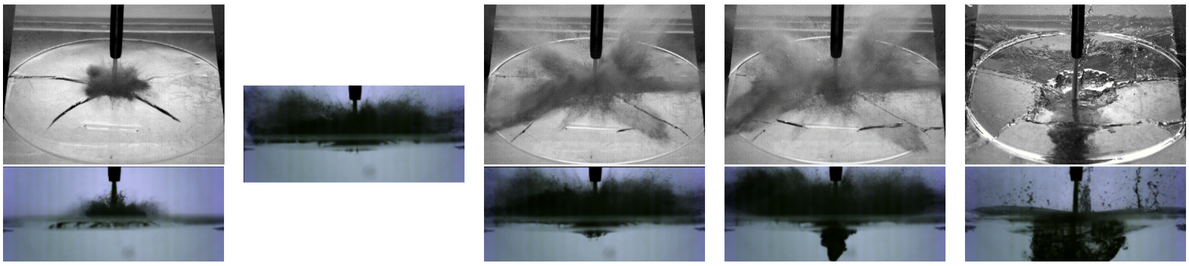
(a) t'=460μs (b) t'=1770μs (t'_{pen}) (c) t'=1910μs (d)t'=2310μs (t'_{com}) (e)t'=20010μs

Fig. 9 Ice plate with initial circumferential defect (I-ICC)

Fig. 9 showed the damage process of ice plate with circumferential defect (I-ICC). Firstly, it could be found that in this case, the damage process of the ice plate was basically the same as that of the intact ice plate, including the expansion of radial cracks and the generation of subsequent circumferential cracks. However, the location of the initial circumferential defect determined the propagation location of the circumferential crack to a certain extent. Besides, the circumferential defect also accelerated the damage process of the ice plate.

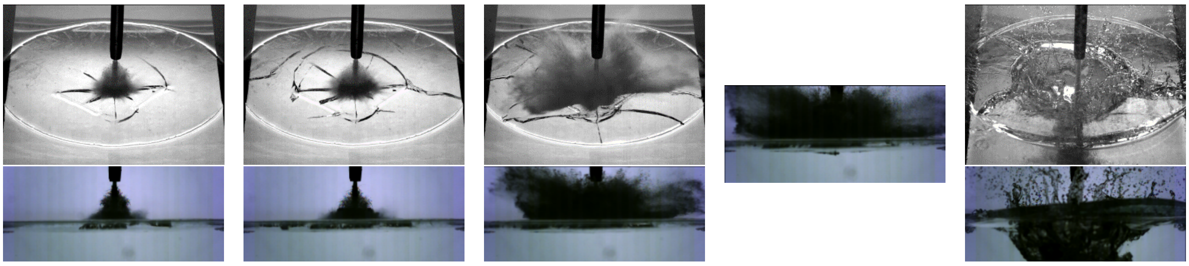
(a) t'=170μs (b) t'=270μs (c) t'=1220μs (t'_{com}) (d)t'=1500μs (t'_{pen}) (e)t'=20020μs

Fig. 10 Ice plate with initial circumferential defect (II-ICCs)


(a) t'=170μs (b) t'=620μs (c) t'=1910μs (t'_{pen}) (d)t'=2520μs (t'_{com}) (e)t'=20020μs

Fig. 11 Ice plate with initial circumferential defect (III-ICCs)

Figs. 10 and 11 showed the effect of initial defects (II-ICCs and III-ICCs) on ice plate damage and crack expansion. The radial cracks gradually expanded and connected with the initial circumferential defect. The existence of the circumferential defects would affect the further propagation of the radial cracks, and the new radial cracks would form at the edge of the initial defect and expand towards the outer edge of the ice plate. Similar to the circumferential defect (I-ICC), the circumferential crack generated at the edge of the initial defect and extended circumferentially along the ice plate. In both cases, the final failure modes and states of the ice plate were basically the same, as shown in Figs.10 (e) and 11 (e). There were both two initial circumferential defects for the cases, but the circumferential defects (II-ICCs) had more obvious accelerating effects on ice plate damage. In other words, under the same loads, ice plate with the circumferential defects (II-ICCs) was more prone to damage.

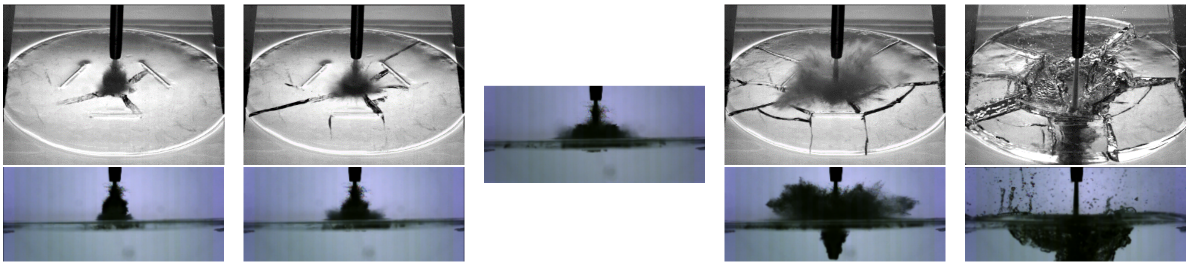
(a) t'=40μs (b) t'=140μs (c) t'=280μs (t'_{pen}) (d)t'=740μs (t'_{com}) (e)t'=20040μs

Fig. 12 Ice plate with initial circumferential defect (IV-ICCs)

Finally, we analyzed the case with three initial circumferential defects, as shown in Fig. 12. The propagation process involving radial and circumferential cracks was similar to the above situation. When the radial crack generated in the center of the ice plate extended to the initial defect, new radial and circumferential cracks were both generated from the edge of the defect and propagated towards the outer edge and circumferential direction of the ice plate. The difference was that the increase in the number of initial defects further speeded up the ice-breaking process. Under the same load, more radial and circumferential cracks were generated, and the final failure state was more intense. In practical engineering applications, for ice of large or infinite size, different initial circumferential defect combinations could be used to to create a breach in the ice. For example, similarly placing multiple initial circumferential crack defects on the ice sheet in advance could more effectively to create gaps in the large-scale ice sheet, combined with the number of initial defects and layout, the size of the ice gap could be improved.

CONCLUSIONS

In this paper, the damage characteristics of high-speed water jet to ice with initial defects were investigated through lab experiments. The focus was the effects of three kinds of initial radial defects and four kinds of initial circumferential defects on the damage and crack propagation of ice plates under high-speed water jet loads. Main conclusions were drawn as below:

1) Under the effect of stagnation pressure of water jet, the radial cracks generated by the initial shock wave were more likely to propagate along the direction of the initial radial defect. The circumferential crack was more likely to propagate from the edge of the initial circumferential defect.
2) Compared with intact ice plates, initial defects could significantly accelerate the damage process of ice plates, and the degree of acceleration was positively correlated with the number of initial defects.
3) In practical engineering application, making initial defects of ice plates artificially is an effective method to improve the ice breaking efficiency. it was suggested to use the initial radial defects to break ice for the small-scale ice plate. For a large-scale ice plate, the combined circumferential defects method could be used to create gaps in the ice.

ACKNOWLEDGEMENTS

This work is supported by the National Natural Science Foundation of China (Nos. 52192693, 52192690, 51979051, 51979056 and U20A20327), and the National Key Research and Development Program of China (2021YFC2803400), to which the authors are most grateful.

REFERENCES

[1] Bazant Z.P., Kim J.J.H., Li Y.N., Part-through bending cracks in sea ice plates: Mathematical modeling. Am.Soc.Mech.Eng.Appl.Mech.Div. 207:97-106(1995).
[2] Bowden F.P., Brunton J.H., The deformation of solids by liquid impact at supersonic speeds. Proc.R.Soc.Lond.Ser.A. 263:433-50(1961).
[3] Ashton, G.D., River and Lake Ice Engineering. Book Craflers. Inc. Chelseas Michigan. USA. 166-174(1986).
[4] Grishina N., Buch V., Structure and dynamics of orientational defects in ice. I.J.Chem.Phys. 120 (11):5217-5225(2004).
[5] Li Z.J., Jia Q., Huang W.F., et al., 2010. Characteristics of ice crystals, gas bubbles and densities of fresh water ice in a reservoir. In: 20th IAHR International Symposium on Ice. Lahti, Finland.
[6] Lu W. et al., Out-of-plane failure of an ice floe: Radial-crack-initiation-controlled fracture. Cold.Reg.Sci.Technol. 119: 183-203(2015).
[7] Moslet P.O., 2007. Field testing of uniaxial compression strength of columnar sea ice. Cold Reg. Sci. Technol. 48 (1), 1-14.
[8] Ni B.Y., Pan Y.T., Yuan G.Y., Xue Y.Z., An experimental study on the interaction between a bubble and an ice floe with a hole. Cold.Reg.Sci.Technol. 187:103281(2021).
[9] Ni B.Y., Wu Q.G., Auxiliary Icebreaking Methods. In Cui W., Fu S., Hu Z.(eds). Encyclopedia of Ocean Engineering. Springer, Singapore (2020).
[10] Ni B.Y., Wei H.Y., Li Z.Y., Fang B., Xue Y.Z., Numerical simulation of an air-bubble system for ice resistance reduction, J. Mar. Sci. Eng.10(9):1201(2022).
[11] Ni B.Y., Tan H., Di S.C., Zhang C.X., Li Z.Y., Huang L., Xue Y.Z. When Does a Light Sphere Break Ice Plate Most by Using Its Net Buoyancy J. Mar. Sci. Eng. 11(2):289(2023).
[12] Riska K., Design of ice breaking ships. In Encyclopedia of Life Support Systems. The EOLSS International Editorial Council. UNESCO (2011).
[13] Sanderson, T. J. O. (1988). Ice mechanics and risks to offshore structures.
[14] Sodhi D.S., Deflection Analysis of Radially Cracked Floating Ice Sheets. OMAE. (1996)
[15] Schulson E.M. and Duval P., Creep and fracture of ice. Cambridge, Cambridge University Press (2009).
[16] Timco G.W., Weeks W.F., A review of the engineering properties of sea ice. Cold.Reg.Sci.Technol. 60(2):107-129(2010).
[17] Wang Y., Zou Z.J., Wang F., Shi C., Luo Y., Lu T.C., A simulation study on the ice fracture behaviors in ice-lighthouse interaction considering initial defects in ice sheet. Ocean.Eng. 173:433-449(2019).
[18] Xue Y.Z., Liu R.W., Li Z., Han D.F., A review for numerical simulation methods of ship-ice interaction. Ocean.Eng. 215:107853(2020).
[19] Yang B.Y., Sun Z., Zhang G.Y., Wang Q.K., Zong Z., Li Z.J., Numerical estimation of ship resistance in broken ice and investigation on the effect of floe geometry. Marine Structures, 75(2021):102867.
[20] Yuan G.Y., Ni B.Y., Wu Q.G., Xue Y.Z., Zhang A.M., An experimental study on the dynamics and damage capabilities of a bubble collapsing in the neighborhood of a floating

ice cake. J.Fluids.Struct. 92:102833(2020).

[21] Yuan G.Y., Ni B.Y., Wu Q.G., Xue Y.Z., Han D.F., Ice breaking by a high-speed water jet impact. J. Fluid. Mech. 934 (2022).